Published in final edited form as:
Exp Neurol. 2011 December ; 232(2): 333–338. doi:10.1016/j.expneurol.2011.09.005.

PET Imaging for Attention Deficit Preclinical Drug Testing in Neurofibromatosis-1 Mice

Jacquelyn A. Brown[a], **Jinbin Xu**[b], **Kelly A. Diggs-Andrews**[a], **David F. Wozniak**[c], **Robert H. Mach**[b], and **David H. Gutmann**[a,*]

[a]Department of Neurology, Washington University School of Medicine, St. Louis MO, USA

[b]Department of Radiology, Washington University School of Medicine, St. Louis MO, USA

[c]Department of Psychiatry, Washington University School of Medicine, St. Louis MO, USA

Abstract

Attention system abnormalities represent a significant barrier to scholastic achievement in children with neurofibromatosis-1 (NF1). Using a novel mouse model of NF1-associated attention deficit (ADD), we demonstrate a presynaptic defect in striatal dopaminergic homeostasis and leverage this finding to apply [^{11}C]-raclopride positron-emission tomography (PET) in the intact animal. While methylphenidate and L-Deprenyl correct both striatal dopamine levels on PET imaging and defective attention system function in *Nf1* mutant mice, pharmacologic agents that target de-regulated cyclic AMP and RAS signaling in these mice do not. These studies establish a robust preclinical model to evaluate promising agents for NF1-associated ADD.

Keywords

dopamine; behavior; neurofibromin; cyclic AMP; RAS

Introduction

Children with the neurofibromatosis-1 (NF1) inherited cancer syndrome are prone to the development of benign and malignant tumors (Gutmann et al., 1997). However, the most prevalent neurologic problem in children reflects deficits in attention, such that 60–80% of affected individuals exhibit ADD symptomatology (Hyman et al., 2005). To define the neurochemical basis for NF1-associated attention deficits, we employed a unique *Nf1* genetically-engineered mouse (GEM) model (Brown et al., 2010a). These *Nf1* mutant mice demonstrate reduced exploratory behaviors, as well as selective and non-selective attention abnormalities, where the non-selective attention deficit was restored to wild-type levels following treatment with methylphenidate (MPH) or L-Dopa. Consistent with this pharmacologic correction, *Nf1* mutant mice have reduced striatal dopamine levels revealed by high-performance liquid chromatography (HPLC).

*Corresponding author: David H. Gutmann, MD, PhD, Department of Neurology, Box 8111; 660 South Euclid Avenue, Saint Louis MO 63110. 314-362-7379 (Phone), 314-362-2388 (FAX); gutmannd@neuro.wustl.edu.

To translate these basic research findings to a preclinical therapeutic drug testing platform, we applied neurotransmitter imaging methods and behavioral analyses to monitor this dopaminergic deficit in the intact animal. In the current study, we establish that this dopaminergic defect in *Nf1* mutant mice is presynaptic, and can be quantified by [^{11}C]-raclopride PET imaging. We further demonstrate that correction of a non-selective attention deficit in *Nf1* mutant mice with MPH and L-Deprenyl correlates with normalization of raclopride binding *in vivo*, whereas therapies that target NF1-regulated RAS and cyclic AMP (cAMP) defects in these mice correct neither the behavioral nor the imaging abnormalities.

Materials and Methods

Mice

Nf1+/−^{GFAP}CKO (CKO) and control littermate *Nf1*$^{flox/flox}$ (WT) mice were maintained on an inbred C57BL/6 background (Bajenaru et al., 2003; Brown et al., 2010a) with *ad libitum* access to food and water. *Nf1*+/−^{GFAP}CKO mice are *Nf1*+/− mice (reduced *Nf1* gene expression in all cells in the brain and body) which harbor complete *Nf1* gene loss in GFAP-expressing cells. All experiments were performed on 3–4 month old mice under active Animal Studies Committee protocols. Independently-generated groups of WT and CKO mice were used for the baseline PET imaging studies (Fig. 1), MPH and L-Deprenyl treatments (Fig. 2), and Lovastatin and Rolipram treatments (Fig. 3).

Radioligand and compound preparation

[^{3}H]-SCH23390, [^{3}H]-raclopride, [^{3}H]-Win 35428 (PerkinElmer Life and Analytical Sciences; Shelton, CT), [^{3}H]-WC-10, and [^{3}H]-a-Dihydrotetrabenazine ([^{3}H]-DTBZ; American Radiolabeled Chemicals; St. Louis, MO) were used as previously reported (Xu et al., 2009).

Quantitative receptor autoradiography

20-micron coronal sections were generated from flash-frozen brains and processed for autoradiography as previously described (Xu et al., 2009; Xu et al., 2010). Sections were incubated for 60 min at room temperature with [^{3}H]-SCH23390 (D1 receptors), [^{3}H]-raclopride (D2 receptors), [^{3}H]-WC-10 (D3 receptors), [^{3}H]-DTBZ (VMAT2), or [^{3}H]-Win 35428 (DAT) (Frey et al., 1997; Savasta et al., 1986; Xu et al., 2010). Non-specific binding was determined following the addition of 1μM (+)-butaclamol, 1μM eticlopride, 1μM tetrabenazine, or 1μM nomifensine, respectively. Quantitation was performed using the Beta Imager 2000Z Digital Beta Imaging System (Biospace, France) and the Beta-Vision Plus program (Xu et al., 2010).

Small animal PET analysis

Brain PET imaging was performed under isoflurane anesthetization. Mice were injected with ~200μCi of [^{11}C]-raclopride (~2500 Ci/mmol specific activity) *via* the tail vein and data acquired as 1h dynamic scans using the Siemens Focus F220 and Inveon scanners (Siemens Medical Solutions USA, Inc.). Acquired list mode data were converted into a 3D set of sinograms and binned into 5 × 60-sec, 5 × 2-min and 9 × 5-min time frames for processing using filter back projection algorithm with attenuation and scatter corrections. Using 5–60min summarized PET images and co-registered CT images as references, regions of interest (ROI) for the striatum and cerebellum were manually drawn with the software Acquisition Sinogram Image PROcessing using IDL's Virtual Machine™ (ASIPro VM™) to obtain radioactivity uptake (nCi/c.c.) curves over time. Representative PET and CT co-registration images are shown in Supplementary Fig. 1A and 1B, respectively. Logan

DVR-1 (binding potential) analyses were performed using the cerebellum as the reference region, with a K2 value of 0.2 (Logan, 2000).

Drug treatments

Mice received intraperitoneal (i.p.) injections of sterile water (vehicle), MPH (20mg/kg; Sigma) or L-Deprenyl (10mg/kg; Sigma) the day before and on the day of testing, and evaluated 45min after last injection or injected once with MPH and tested immediately after injection (Brown et al., 2010a; Vallone et al., 2002). Rolipram (5mg/kg/day; Sigma) was delivered via oral gavage for two weeks before testing (Brown et al., 2010b), while Lovastatin (10mg/kg; Sigma) was administered as a single injection 15min before testing (Li et al., 2005).

Behavioral studies

Responses to a novel environment were evaluated over a 1h period using computerized photobeam instrumentation as previously described (Brown et al., 2010a; Vallone et al., 2002). General ambulatory activity (total ambulations or whole body movements) and vertical rearing, a component of non-selective attention (i.e., orienting) were quantified. Mice used for the behavioral studies were the same mice examined by PET imaging.

Immunohistochemistry and Western blotting

Western blots and immunohistochemistry (IHC) using DARPP32, p-MAPK, total MAPK (Cell Signaling) and p-DARPP32 (Abcam) antibodies were performed as previously described (Dasgupta et al., 2005). cAMP measurements were determined by ELISA (Brown et al., 2010b). Each experiment was performed using samples from at least three independent cohorts of mice.

Results

Nf1 CKO mice have a presynaptic striatal dopamine defect

Our previous experiments using *Nf1* CKO mice revealed a 10% reduction in the number of *Nf1*+/− tyrosine hydroxylase (TH)-positive neurons innervating the striatum *in vivo* as well as a cell-autonomous 50% decrease in neurite length *in vitro*, suggesting a presynaptic defect (Brown et al., 2010a). To establish a presynaptic dopamine (DA) defect relevant to preclinical drug testing, we performed two additional experiments. Using IHC (Fig. 1A) and Western blotting (Fig. 1B), we found reduced DARPP32 phosphorylation, a key protein activated by DA release, in the striatum of CKO mice (Fisone et al., 2007). Second, using quantitative autoradiography, we demonstrate a 10% reduction in the expression of presynaptic (VMAT2 and DAT) DA transporters, but normal expression of postsynaptic D1, D2, and D3 receptors (Fig. 1C–D) (p=.03, p=.0004; N=6). Together with our earlier findings, these data provide direct evidence that the decreased striatal DA levels result from a presynaptic defect with preservation of postsynaptic DA receptor expression.

MPH and L-Deprenyl correct the reduced post-synaptic dopamine receptor occupancy defect revealed by [^{11}C]-raclopride PET imaging

The presence of normal postsynaptic DA receptor densities in CKO mice with attention deficits suggests that PET imaging methods which quantify the levels of postsynaptic dopamine receptor occupancy would serve as surrogate measures of striatal DA levels in the intact mouse. Using [^{11}C]-raclopride PET imaging, we confirmed the 40% reduction in striatal DA levels originally measured by HPLC (Brown et al., 2010a) in CKO mice relative to their WT littermate controls (Fig. 1E–G). Representative Logan plots and PET images are

shown in Fig. 1E and Fig. 1F, respectively. The mean DVR-1 values for all mice (WT and *Nf1* CKO mice; N=4 per genotype) are graphically illustrated in Fig. 1G.

We then leveraged these findings to determine whether MPH treatment restored normal [^{11}C]-raclopride levels in CKO mice. Using MPH doses which we have been previously shown to increase exploratory activity and rearing (Brown et al., 2010a), [^{11}C]-raclopride binding in CKO mice was reduced to WT levels (Fig. 2A–C). As above, representative Logan plots and PET images are shown in Fig. 2A and Fig. 2B, respectively, while the mean DVR-1 values for CKO mouse treatment groups are graphically illustrated in Fig. 2C. Next, we examined the ability of L-Deprenyl, a monoamine oxidase-B inhibitor that prevents the breakdown of DA, to correct the dopamine and behavioral defects in CKO mice. Similar to MPH and L-Dopa (Brown et al., 2010a), L-Deprenyl treatment restored the [^{11}C]-raclopride levels to WT levels (Fig. 2A–C) as well as increased exploratory behavior (Fig. 2D) and significantly improved a component of non-selective attention (Fig. 2E).

Preclinical evaluation of biologically-based treatments

The ability to accurately measure striatal DA levels in the intact mouse coupled with a robust exploratory behavior (attention deficit) screen lay the foundations for preclinical drug studies that target NF1 (neurofibromin)-specific signaling pathways. We focused on the two major neurofibromin signaling pathways deregulated in the brains of CKO mice, intracellular cAMP levels and RAS activation (Brown et al., 2010b; Costa et al., 2002; Dasgupta et al., 2005; Tong et al., 2002). Reduced *Nf1* expression leads to decreased brain cAMP levels (Brown et al., 2010; Warrington et al., 2007), which can be restored to WT levels following treatment with the phosphodiesterase inhibitor, Rolipram (Fig. 3A). Similarly, reduced neurofibromin expression results in increased brain RAS activation (Dasgupta et al., 2005), which is attenuated after treatment with the HMG-CoA reductase inhibitor, Lovastatin (Li et al., 2005), using MAPK activation as a surrogate marker for RAS activity (Fig. 3B). Despite good target inhibition, neither therapy normalized striatal [^{11}C]-raclopride binding (Fig. 3C–D), increased ambulatory activity (Fig. 3E), or improved non-selective attention in CKO mice (Fig. 3F).

Discussion

While NF1 is largely regarded as a tumor predisposition syndrome, 60% of children with NF1 exhibit abnormalities in attention system dysfunction which negatively impact overall scholastic performance. While MPH and related stimulant medications are efficacious in some children with NF1, there is a pressing need to identify and evaluate additional treatment strategies. In this report, we translate our basic science finding of reduced striatal DA levels to preclinical drug testing studies using [^{11}C]-raclopride PET (Schiffer et al., 2006; Thanos et al., 2002). In proof of concept experiments, we show that agents that elevate DA are effective at correcting PET-measured DA levels and an index of non-selective attention in the same animal. Our results raise several important clinically-relevant issues.

First, we demonstrate that the non-selective attention deficit in *Nf1* mutant mice results from a presynaptic DA defect based on reduced striatal DARPP32 phosphorylation, VMAT2/DAT expression, and [^{11}C]-raclopride binding *in vivo*. Importantly, since postsynaptic DA function is intact, pharmacologic interventions that activate these receptors will likely improve DA-dependent non-selective attention abnormalities as observed following MPH, L-Deprenyl, and L-Dopa treatment. Second, similar to *Nf1* mutant mice, there may be a subgroup of children with NF1-associated learning disabilities who are most likely to respond to DA-targeted therapies. These children might be identified by [^{11}C]-raclopride PET imaging, and pre-selected for treatments that restore normal DA levels. Future studies

could leverage the clinical experience with PET for ADHD in the general population to more effectively personalize treatments for children with NF1 (Rosa-Neto et al., 2005; Volkow et al., 2007; Wang et al., 1999). However, due to the radiation dose associated with PET-CT imaging, this approach may have to be limited to older kids and teens or may need to involve PET-MRI (Kim et al., 2010). Third, pharmacologic approaches that target de-regulated signaling pathways in children with NF1 could be more effectively utilized. Previous studies using *Nf1* mutant mice with spatial learning and memory deficits demonstrated that inhibition of RAS activation using Lovastatin corrected these abnormalities (Li et al., 2005). However, clinical studies using Lovastatin have shown little efficacy (Krab et al., 2008). One possible explanation for this outcome was the use of an unselected population of children with different NF1-associated molecular bases for their cognitive deficiencies. In this regard, it is possible that children with learning problems unresponsive to Lovastatin treatment would respond to DA-targeted therapies. This hypothesis is consistent with our finding that Lovastatin did not enhance the non-selective attention performance of *Nf1* CKO mice. The implementation of imaging as a pre-selection modality facilitates the identification of children within a heterogeneous population of individuals with NF1 to be stratified based on their likelihood of responding to specific targeted therapies.

Conclusion

In this study, we demonstrate that the attention deficit in *Nf1* mutant mice results from a presynaptic defect in striatal dopamine homeostasis, and show that this striatal dopaminergic defect can be detected and quantified in the intact animal using [^{11}C]-raclopride positron emission tomography. Using this preclinical model, we demonstrate that pharmacologic agents which increase striatal dopamine levels (methylphenidate and L-Deprenyl) correct the behavioral and PET imaging deficits in *Nf1* mutant mice *in vivo*. We also show those treatments which restore normal cAMP (rolipram) or RAS (lovastatin) signaling in *Nf1* mutant mice neither correct the behavioral nor the PET imaging deficits *in vivo*. Collectively, these findings establish a robust preclinical platform for the evaluation of promising agents for NF1-associated ADD.

Supplementary Material

Refer to Web version on PubMed Central for supplementary material.

Acknowledgments

We appreciate the technical assistance of the Animal Behavior Core (Joshua Dearborn) and the PET imaging facility. This work was funded by grants from the National Cancer Institute (U01-CA141549; DHG), Department of Defense (NF093033; DHG and DFW), and by a National Institute of Child Health and Human Development Center Grant, P30 HD062171 (DFW) and a Pilot Research Grant from the Mallinckrodt Institute of Radiology.

Abbreviations

ADD	Attention Deficit Disorder
cAMP	cyclic adenosine monophosphate
CKO	conditional knockout
CT	computerized tomography
DA	dopamine
GEM	genetically-engineered mouse

MPH	methylphenidate
PET	positron emission tomography

References

Bajenaru ML, Hernandez MR, Perry A, Zhu Y, Parada LF, Garbow JR, Gutmann DH. Optic nerve glioma in mice requires astrocyte Nf1 gene inactivation and Nf1 brain heterozygosity. Cancer Res. 2003; 63:8573–8577. [PubMed: 14695164]

Brown JA, Emnett RJ, White CR, Yuede CM, Conyers SB, O'Malley KL, Wozniak DF, Gutmann DH. Reduced striatal dopamine underlies the attention system dysfunction in neurofibromatosis-1 mutant mice. Hum Mol Genet. 2010a; 19:4515–4528. [PubMed: 20826448]

Brown JA, Gianino SM, Gutmann DH. Defective cAMP generation underlies the sensitivity of CNS neurons to neurofibromatosis-1 heterozygosity. J Neurosci. 2010b; 30:5579–5589. [PubMed: 20410111]

Costa RM, Federov NB, Kogan JH, Murphy GG, Stern J, Ohno M, Kucherlapati R, Jacks T, Silva AJ. Mechanism for the learning deficits in a mouse model of neurofibromatosis type 1. Nature. 2002; 415:526–530. [PubMed: 11793011]

Dasgupta B, Yi Y, Chen DY, Weber JD, Gutmann DH. Proteomic analysis reveals hyperactivation of the mammalian target of rapamycin pathway in neurofibromatosis 1-associated human and mouse brain tumors. Cancer Res. 2005; 65:2755–2760. [PubMed: 15805275]

Fisone G, Hakansson K, Borgkvist A, Santini E. Signaling in the basal ganglia: postsynaptic and presynaptic mechanisms. Physiol Behav. 2007; 92:8–14. [PubMed: 17585965]

Frey K, Kilborn M, Robinson T. Reduced striatal vesicular monoamine transporters after neurtotoxic but not after behaviorally-sensitizing doses of methamphetamine. Eur J Pharmacol. 1997; 334:273–279. [PubMed: 9369358]

Gutmann DH, Aylsworth A, Carey JC, Korf B, Marks J, Pyeritz RE, Rubenstein A, Viskochil D. The diagnostic evaluation and multidisciplinary management of neurofibromatosis 1 and neurofibromatosis 2. JAMA. 1997; 278:51–57. [PubMed: 9207339]

Hyman SL, Shores A, North KN. The nature and frequency of cognitive deficits in children with neurofibromatosis type 1. Neurology. 2005; 65:1037–1044. [PubMed: 16217056]

Kim S, Salamon N, Jackson HA, Bluml S, Panigraphy A. PET imaging in pediatric neuroradiology: current and future applications. Pediatr Radiol. 2010; 40:82–96. [PubMed: 19937235]

Krab LC, de Goede-Bolder A, Aarsen FK, Pluijm SM, Bouman MJ, van der Geest JN, Lequin M, Catsman CE, Arts WF, Kushner SA, Silva AJ, de Zeeuw CI, Moll HA, Elgersma Y. Effect of simvastatin on cognitive functioning in children with neurofibromatosis type 1: a randomized controlled trial. JAMA. 2008; 300:287–294. [PubMed: 18632543]

Li W, Cui Y, Kushner SA, Brown RA, Jentsch JD, Frankland PW, Cannon TD, Silva AJ. The HMG-CoA reductase inhibitor lovastatin reverses the learning and attention deficits in a mouse model of neurofibromatosis type 1. Curr Biol. 2005; 15:1961–1967. [PubMed: 16271875]

Logan J. Graphical analysis of PET data applied to reversible and irreversible tracers. Nucl Med Biol. 2000; 27:661–670. [PubMed: 11091109]

Rosa-Neto P, Lou HC, Cumming P, Pryds O, Karrebaek H, Lunding J, Gjedde A. Methylphenidate-evoked changes in striatal dopamine correlate with inattention and impulsivity in adolescents with attention deficit hyperactivity disorder. Neuroimage. 2005; 25:868–876. [PubMed: 15808987]

Savasta M, Dubois A, Scatton B. Autoradiographic localization of D1 dopamine receptors in the rat brain with [3H]SCH 23390. Brain Res. 1986; 375:291–301. [PubMed: 2942221]

Schiffer WK, Volkow ND, Fowler JS, Alexoff DL, Logan J, Dewey SL. Therapeutic doses of amphetamine or methylphenidate differentially increase synaptic and extracellular dopamine. Synapse. 2006; 59:243–251. [PubMed: 16385551]

Thanos PK, Taintor NB, Alexoff D, Vaska P, Logan J, Grandy DK, Fang Y, Lee JH, Fowler JS, Volkow ND, Rubinstein M. In vivo comparative imaging of dopamine D2 knockout and wild-type

mice with (11)C-raclopride and microPET. J Nucl Med. 2002; 43:1570–1577. [PubMed: 12411561]

Tong J, Hannan F, Zhu Y, Bernards A, Zhong Y. Neurofibromin regulates G protein-stimulated adenylyl cyclase activity. Nat Neurosci. 2002; 5:95–96. [PubMed: 11788835]

Vallone D, Pignatelli M, Grammatikopoulos G, Ruocco L, Bozzi Y, Westphal H, Borrelli E, Sadile AG. Activity, non-selective attention and emotionality in dopamine D2/D3 receptor knock-out mice. Behav Brain Res. 2002; 130:141–148. [PubMed: 11864730]

Volkow ND, Wang GJ, Newcorn J, Telang F, Solanto MV, Fowler JS, Logan J, Ma Y, Schulz K, Pradhan K, Wong C, Swanson JM. Depressed dopamine activity in caudate and preliminary evidence of limbic involvement in adults with attention-deficit/hyperactivity disorder. Arch Gen Psychiatry. 2007; 64:932–940. [PubMed: 17679638]

Wang GJ, Volkow ND, Fowler JS, Logan J, Pappas NR, Wong CT, Hitzemann RJ, Netusil N. Reproducibility of repeated measures of endogenous dopamine competition with [11C]raclopride in the human brain in response to methylphenidate. J Nucl Med. 1999; 40:1285–1291. [PubMed: 10450679]

Warrington NM, Woerner BM, Dagninakatte GC, Dasgupta B, Perry A, Gutmann DH, Rubin JB. Spatiotemporal differences in CXCL12 expression and cyclic AMP underlie the unique pattern of optic glioma growth in neurofibromatosis type 1. Cancer Res. 2007; 67:8588–8595. [PubMed: 17875698]

Xu J, Chu W, Tu Z, Jones LA, Luedtke RR, Perlmutter JS, Mintun MA, Mach RH. [(3)H]4-(Dimethylamino)-N-[4-(4-(2-methoxyphenyl)piperazin- 1-yl)butyl]benzamide, a selective radioligand for dopamine D(3) receptors. I. In vitro characterization. Synapse. 2009; 63:717–728. [PubMed: 19425052]

Xu J, Hassanzadeh B, Chu W, Tu Z, Jones LA, Luedtke RR, Perlmutter JS, Mintun MA, Mach RH. [3H]4-(dimethylamino)-N-(4-(4-(2-methoxyphenyl)piperazin-1-yl) butyl)benzamide: a selective radioligand for dopamine D(3) receptors. II. Quantitative analysis of dopamine D(3) and D(2) receptor density ratio in the caudate-putamen. Synapse. 2010; 64:449–459. [PubMed: 20175227]

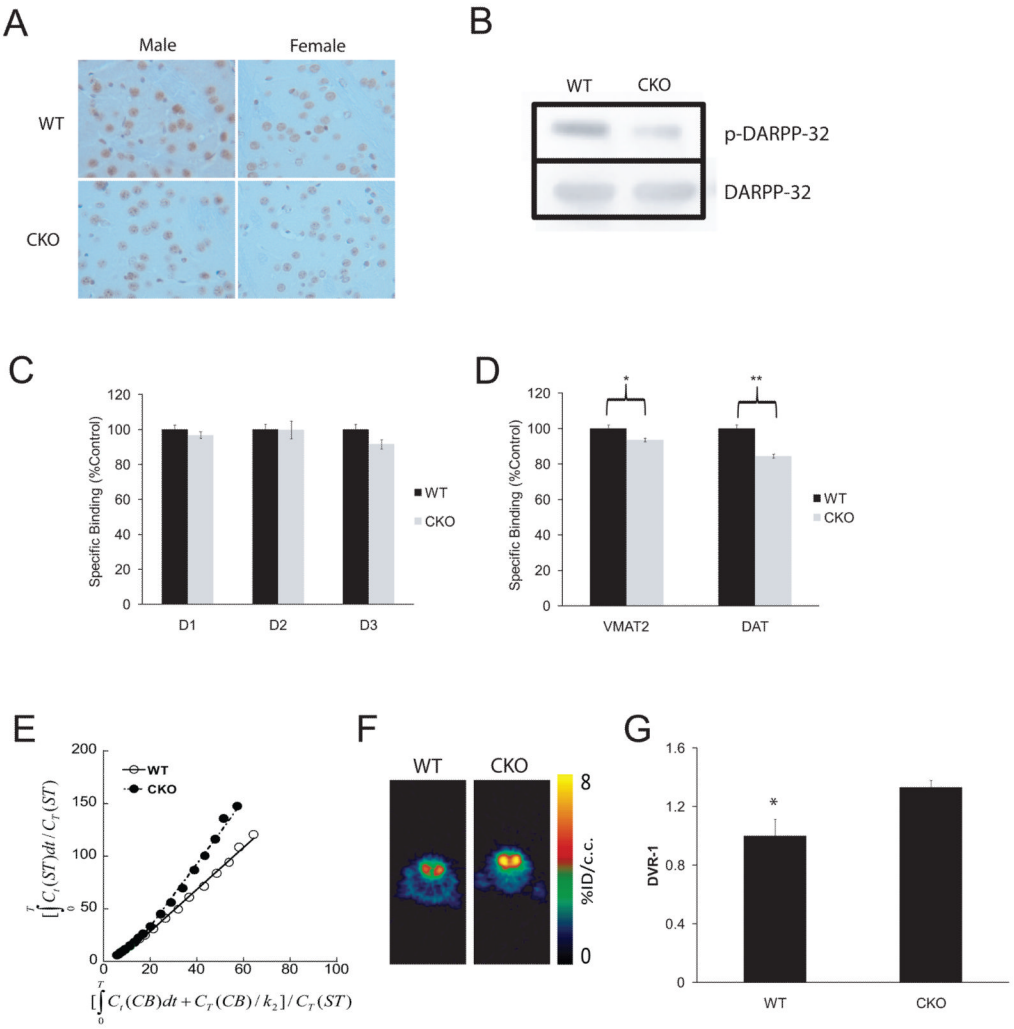

Fig. 1. *Nf1* CKO mice with attention system defects demonstrate a presynaptic DA defect, which can be visualized by PET imaging

(A) IHC reveals decreased DARPP32 phosphorylation (p-DARPP32) in the striatum of both male and female mice relative to WT littermates (p=.01; N=8). **(B)** Western blot shows a 5.8-fold decrease in p-DARPP32 (following normalization to total DARPP32 levels) in CKO compared to WT mice. *In vitro* quantitative receptor autoradiography demonstrates no change in postsynaptic D1, D2 and D3 DA receptor expression in CKO mice relative to control WT littermates **(C)**, whereas presynaptic VMAT2 and DAT expression is reduced (**D**; ~10%; p=.03, VMAT2, p=.0004, DAT; N=6). **(E)** Representative Logan plots for WT and CKO mice (using the cerebellum as the reference region) are shown along with (**F**) representative [^{11}C]-raclopride transverse micro-PET images (summed across 5–60 minutes). The colorscale bar indicates the normalized peak uptake (percent injected dose per cubic centimeter tissue; %ID/cc). (**G**) In a cohort of WT and CKO mice, [^{11}C]-raclopride binding was increased in the striatum (Str) of CKO mice compared to control WT littermates on PET imaging (p=.03; N=4 per genotype). C_t = tissue radioactivity at time t; T = time point of each frame of PET scanning course.

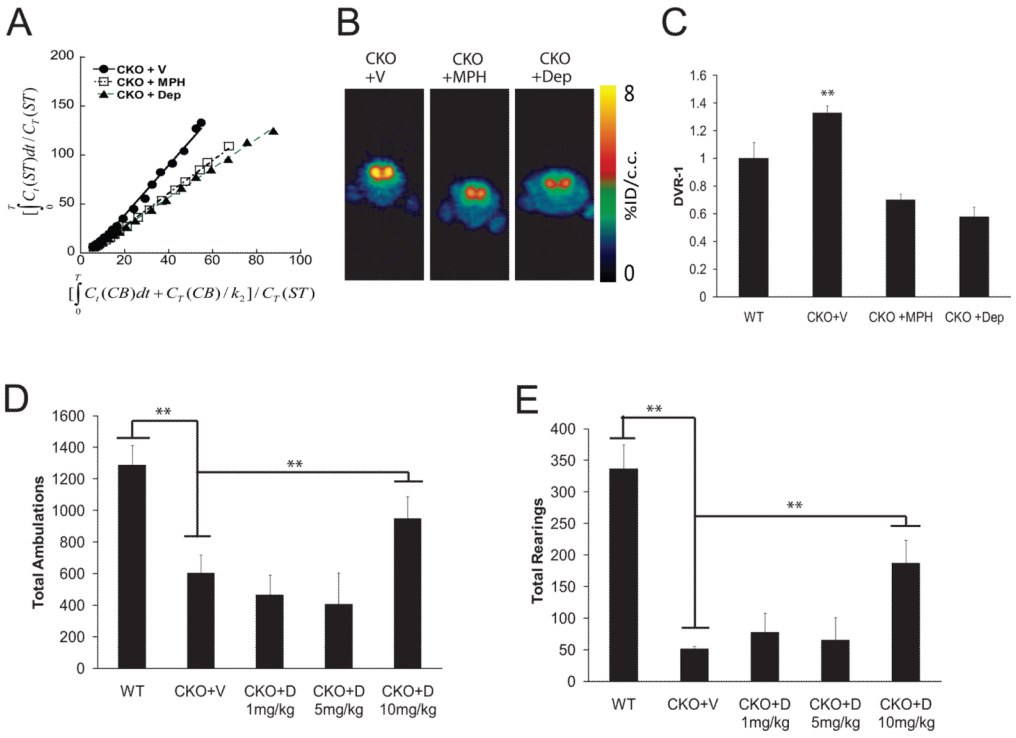

Fig. 2. MPH and L-Deprenyl treatments restore [^{11}C]-raclopride binding and improve exploratory and attention behaviors

(A) Representative Logan plots and (**B**) [^{11}C]-raclopride transverse PET images (summed across 5–60 minutes) of vehicle-treated CKO mice and CKO mice following MPH and L-Deprenyl administration are shown. The colorscale bar indicates the normalized peak uptake (percent injected dose per cubic centimeter tissue; %ID/cc). (**C**) In these experiments, both MPH and Deprenyl reduced [^{11}C]-raclopride binding in the striatum to WT levels (p=.02, p=.005; N=4). C_t = tissue radioactivity at time t; T = time point of each frame of PET scanning course. During a 1h exploration of a novel environment, total ambulations (**D**; p=.02; N=8) and total rearings (a measure of non-selective attention) were increased in CKO mice (**E**; p=.0001; N=8) beyond Bonferonni correction (p=.05/4=.0125) following L-Deprenyl (CKO+D; 10mg/kg) treatment. All mice used for the PET imaging experiments also underwent behavioral testing. Additional independently-generated WT and CKO mice, which did not undergo PET imaging, were included in the behavioral experiments.

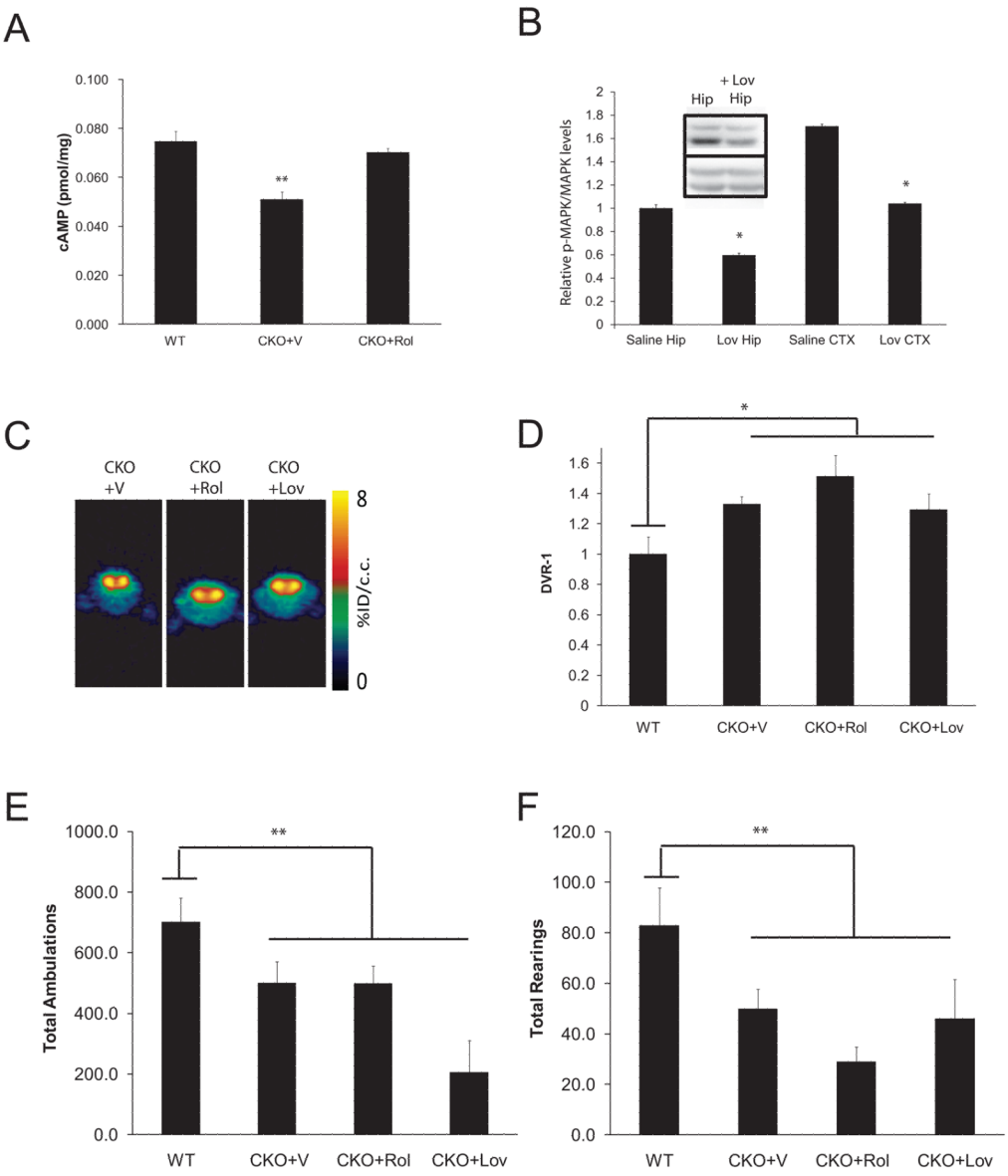

Fig. 3. Biologically-based neurofibromin therapies did not correct the DA defect or attentional deficit in CKO mice

(A) Rolipram (CKO+Rol; 5mg/kg/day × 2 weeks) treatment restored cAMP levels in the striatum of 3-month-old mice. **(B)** Lovastatin (Lov; 10mg/kg i.p.) reduced MAPK activation (p-MAPK) in the cortex (CTX) and hippocampus (Hip) of CKO mice following normalization to total MAPK expression (p=.001; N=3). All fold changes (relative pMAPK/MAPK levels) are relative to saline-treated (vehicle; V) hippocampal levels. Inset shows a representative Western blot for p-MAPK and MAPK in the hippocampus (Hip) following saline and Lovastatin administration. **(C)** Representative [^{11}C]-raclopride transverse micro-PET images (summed across 5–60 minutes) of CKO mice at baseline (vehicle-treated; V) and following Rolipram (Rol) and Lovastatin (Lov) treatment. The colorscale bar indicates the normalized peak uptake (percent injected dose per cubic centimeter tissue; %ID/cc). **(D)** Neither Rolipram nor Lovastatin reduced striatal [^{11}C]-raclopride binding in CKO mice (N=8, N=4). During a 1h exploration of a novel environment, total ambulations (**E**) and total rearings (**F**) show no improvement in CKO mice following Rolipram or Lovastatin

treatment. All mice used for the PET imaging experiments also underwent behavioral testing. Additional independently-generated WT and CKO mice, which did not undergo PET imaging, were included in the behavioral experiments.